

Optimal Path Planning with Clothoid Curves for Passenger Comfort

Edward Derek Lambert^a, Richard Romano^b and David Watling^c
Institute for Transport Studies, University of Leeds, 34-40 University Road, Leeds, U.K.

Keywords: Passenger Comfort, Clothoid, Path Planning, Automated Vehicle.

Abstract: Highly automated vehicles operating at SAE automation level 4 and 5 will not require the occupants' attention to be on the road at all. They will be free to amuse themselves as passengers. This will have the side effect of making them more vulnerable to motion sickness. Automated vehicles must plan paths which are feasible for the vehicle and comfortable for its occupants. In railway and highway design, paths with clothoid based transitions provide feasibility and comfort. This paper proposes a method for generating such a path using constrained non-linear optimization and compares it to an existing method based on root finding.

1 INTRODUCTION

Smooth paths for Automated Vehicles are important for ensuring dynamic feasibility (LaValle and Leidner, 2006a) and passenger comfort (Elsner, 2018). Numerous representations have been developed to accompany different planning algorithms (LaValle and Leidner, 2006b), (Katrakazas et al., 2015), (Paden et al., 2016), (Schwarting et al., 2018). These include cubic splines (Deits and Tedrake, 2015), combinations of lines and arcs with minimum length (Dubins, 1957) and (Reeds and Shepp, 1990), parametric continuous curvature paths (Fraichard and Scheuer, 2004) or clothoids (Wilde, 2009).

Considerable work has been done to develop empirical measures which correlate well with passenger comfort. Generally, acceleration and sometimes its derivative *jerk* are taken to cause physical discomfort if they exceed some threshold. The effect of high acceleration on the human body is well known from studies undertaken on pilots and astronauts: *g*-forces are certainly noticeable and at a high level will eventually lead to unconsciousness and death (McKenney, 1970). At more modest levels acceleration is detected by the inner ear and can lead to motion sickness (Beard and Griffin, 2014). The problems associated with excessive *jerk* are more difficult to quantify but in certain circumstances, such as very short duration motions they can be strongly associated with physical

discomfort (McKenney, 1970). There are also psychological factors which may come into play when riding in an automated vehicle such as perceived risk. Some of these can be taken into account at the planning stage such as keeping a sufficient distance from obstacles to which a human driver would be able to respond (Elsner, 2018).

Based on the assumption that keeping acceleration and its rate of change tightly bounded, while maintaining sufficient distance from any obstruction, leads to maximum passenger comfort, it is possible to evaluate some of the different path representations. All path requirements can be met with any representation, the difference is the efficiency with which the relevant parameters can be evaluated. For the cubic spline the position and derivatives can be evaluated cheaply to check obstacle constraints are satisfied but the curvature rate or sharpness must be derived from samples along the curve once it is plotted. This is similar to the way the curvature of existing roads can be measured based on a series of samples along them (Zamfir et al., 2016). For a clothoid the curvature rate (sharpness) is the defining parameter so it is cheap to evaluate for each section, however the position must be computed by evaluating Fresnel integrals (Wilde, 2009).

Clothoid curves have been in use for a long time in the design of highway and railway easement curves to transition between straight and curved sections comfortably and safely (Levien, 2008). For this reason we propose that the use of clothoid curves (with an appropriate upper bound on sharpness and curvature) is sufficient to ensure the physical comfort of the occupants without further experimental results, and there-

^a <https://orcid.org/0000-0002-2297-0441>

^b <https://orcid.org/0000-0002-2132-4077>

^c <https://orcid.org/0000-0002-6193-9121>

fore will proceed to address the problem of calculating the parameters for curves of this type which join a given origin and destination as addressed by (Gim et al., 2017) and (Wilde, 2009).

This paper goes on to describe a method for identifying the parameters of a clothoid spline joining two points based on constrained non-linear optimization in Section 4, and compares it to the bisection method proposed by (Gim et al., 2017) detailed in Section 3.

1.1 Appropriate Limits

Correct choice of curvature and curvature rate limit is essential for a smooth ride. The length of easement curve required for a particular turn of curvature $\kappa = 1/R$ is given by

$$s = \kappa/\alpha_{max} \quad (1)$$

Certain parameters have been specified for European Railway Design in ES13803 (Fischer, 2008). These include a maximum cant rate of 50mm/s. Cant is the height of one railway track above another and is related to the path curvature by the requirement the track remain 'balanced' meaning that both rails are loaded equally as a train passes over at design speed.

As a result, maximum sharpness α can be expressed in terms of the cant rate E assuming a balanced track of gauge G and constant traversal speed V .

$$\alpha = \frac{Eg}{V^3G} \quad (2)$$

where g is the acceleration due to gravity, approximately $9.81m/s^2$. The appropriate sharpness to match the cant rate limit is found to be $\alpha_{max} = 4 \times 10^{-5} m^{-2}$. If this rate can be sustained on existing roads without requiring an unacceptable reduction in forward speed, Level 5 autonomy could be as smooth and pleasant environment for work or rest as a typical train journey, along with the additional privacy of car travel.

2 PROBLEM STATEMENT

Given a workspace $W = \mathbb{R}^2$ and an obstacle region $O \subset W$ and a robot defined by a rigid body $A \in W$. Configuration space C can be broken down into C_{obs} and C_{free} . A single query must provide an initial configuration $\mathbf{q}_I \in C_{free}$ and a goal configuration $\mathbf{q}_G \in C_{free}$. The problem is to compute a continuous path over $\tau : [0, L] \rightarrow C_{free}$ such that $\tau(0) = \mathbf{q}_I$ and $\tau(L) = \mathbf{q}_G$

This is also known as the piano mover's problem, for more details see (Siciliano and Khatib, 2016). A car can be treated as a rigid body that moves in a plane

with a state $\mathbf{x} = [x, y, \psi]$ where x and y indicate position of the vehicle control point in the 2D plane and ψ is the forward direction of the vehicle, measured anticlockwise from the x -axis. Configuration space has dimension $C = \mathbb{R}^2 + S^1$.

We place an additional restriction that the path τ must have piecewise constant sharpness $\alpha = d^2\psi/ds^2 \leq \alpha_{max}$ so it takes the form of a clothoid spline. The peak curvature must also be less than a comfortable maximum $\kappa = d\psi/ds \leq \kappa_{max}$

3 METHOD 1: BISECTION

One approach to generating true clothoid curves between two positions is based on root finding. A general approach for creating parametrized Continuous Curvature Paths (pCCP) based on clothoids is detailed in (Gim et al., 2017). The process begins with a discrete set of samples, such as could be produced by a lattice planner which did not take into account differential constraints. Central to this approach is the identification of the parameters sharpness α_1 and deflection δ_1 describing a matched clothoid pair which terminates at a specified $\mathbf{x}_G = [x_G, y_G, \psi_G]$, $\kappa_G=0$. The constraint on heading and curvature can be used to calculate the sharpness and deflection of the second clothoid segment from the first. The terminating position can be found by evaluating the Fresnel integrals to find the 2D position error with respect to \mathbf{q}_G . The error can be expressed relative to the end of the clothoid pair to get the forward and lateral components. There is then a two dimensional root finding process based on bisection to arrive at the parameter values which drive lateral error to zero.

A single clothoid segment parametrized in s is defined by the a constant sharpness $\alpha = d^2\psi/ds^2$ along its length. States on the path $\tau(s) = [x(s), y(s), \psi(s), \kappa(s)]$ can be found by evaluating the Fresnel integrals.

$$\kappa(s) = \alpha s \quad (3)$$

$$\psi(s) = \frac{\alpha s^2}{2} \quad (4)$$

$$x(s) = \int_0^s \cos\psi(u) du \quad (5)$$

$$y(s) = \int_0^s \sin\psi(u) du \quad (6)$$

The result is a spiral shown in Figure 1. As an easement curve, the most useful section is close to the origin where the curvature is low and it is well approximated by a cubic.

It is possible to construct a continuous curvature path starting and ending with a straight line using two

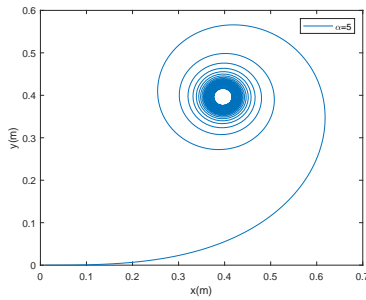


Figure 1: A clothoid spiral with sharpness constant $\alpha = 5$.

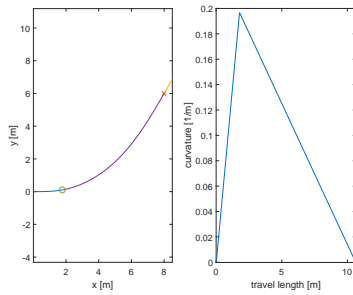


Figure 2: A matched pair of clothoids suitable for joining two straight lines.

matched clothoid curves, one increasing the curvature and the other decreasing it to maintain continuity. This construction is shown in Figure 2. This gives rise to some analytic relations between the first and second matched clothoid which are reproduced from (Gim et al., 2017).

$$\kappa_1 = \sqrt{2\delta_1\alpha_1} \quad (7)$$

$$\kappa_2 = \kappa_1 \quad (8)$$

$$\delta_2 = \theta_b - \delta_1 \quad (9)$$

$$\alpha_2 = \frac{\kappa_2^2}{2\delta_2} \quad (10)$$

$$s_1 = \sqrt{\frac{2\delta_1}{\alpha_1}} \quad (11)$$

$$s_2 = \sqrt{\frac{2\delta_2}{\alpha_2}} \quad (12)$$

Using these relations and the boundary condition of the starting configuration $\mathbf{q}_I = [x, y, \psi, \kappa] = [0, 0, 0, 0]$ and ending configuration $\mathbf{q}_G = [x_f, y_f, \psi_f, 0]$ the matched pair is fully defined by the sharpness α_1 and deflection δ_1 of the first segment. These parameters can be found as roots of the (signed) lateral error.

The iterative procedure, based on the bisection method for root finding is given below, using the sign convention in Figure 3.

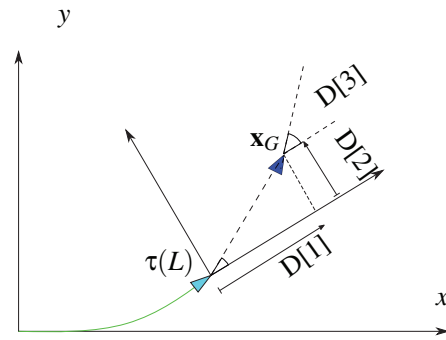


Figure 3: The sign convention used for the forward and lateral error to the goal at the end of the curve.

```

while sol==0 && iter<80
    k1 = sqrt(2*deflection1*alpha1);
    k2 = k1;

    deflection2 = boundary(3) - deflection1;

    alpha2 = k2*k2/(2*deflection2);
    S1 = sqrt(2*deflection1/alpha1);
    S2 = sqrt(2*deflection2/alpha2);

    [x, y, psi, kappa] = clothoid_pair(alpha1,...
        S1, -alpha2, S2);
    n = length(x);

    final_pose = [x(n), y(n), psi(n)];
    D = decompose(boundary(1:3), final_pose);

    DeT = D(1);
    De = D(2);

    iter = iter+1;

    if abs(De)<tol
        if DeT >= 0
            sol=1;
        end
    end
    if lambda*De<0
        dAlpha = dAlpha/2;
    end
    if lambdaT*DeT<0
        dDeflection = dDeflection/2;
    end

    lambda = De;
    lambdaT = DeT;

    dAlpha = abs(dAlpha)*sign(lambda);
    dDeflection = -abs(dDeflection)*sign(lambdaT);

    alpha1 = alpha1 + dAlpha;
    deflection1 = deflection1 + dDeflection;

end
    
```

On careful examination there are a few important differences from bisection as described in a textbook

and the presented method. Convergence is guaranteed of the textbook method for finding a root of a scalar function of one dimension provided a single zero crossing exists within the given interval (Atkinson, 1988). The number of iterations required to reduce the error below a given threshold has an upper bound given by

$$|\alpha - c_n| \leq \left[\frac{1}{2}\right]^n (b - a) \quad (13)$$

where $b - a$ denotes the length of the original interval, c_n is the estimate after n iterations and α is the true value of the root.

The method of (Gim et al., 2017) listed in Verbatim 3 does not require an interval containing the root, only an initial guess smaller than the true value for each parameter because there is an additional search procedure. This relies on knowledge of the direction of relative motion of the end of the path, in the forward and lateral directions based on the two parameters. The justification is detailed in (Gim et al., 2017).

By inspection of the goal pose either two or four clothoids are composed.

$$n_c = \begin{cases} 2 & \text{if } \psi_G > \text{atan2}(y_G, x_G); \\ 4 & \text{if } \psi_G < \text{atan2}(y_G, x_G). \end{cases} \quad (14)$$

The four clothoid case proceeds by searching over the heading of an intermediate point, at each iteration performing the two clothoid estimation twice, once before the intermediate point and once after.

4 METHOD 2: NON-LINEAR OPTIMIZATION

Numerical optimization based path planning is widely used as it leads to 'better' paths, having a lower cost integral over their length with reduced sampling artefacts compared to sampling based methods. The downside of numerical optimization is the higher computational cost to find a path. However, the cost is dependant on the dimension of configuration space, and road vehicles are well served by planning in $C = R^2 + S^1$, which is comparatively low. A good review of planning techniques is given by (Siciliano and Khatib, 2016).

The relations given in Equation 7- 12 are first used to reduce the number of parameters which need to be searched to two, sharpness α_1 and deflection δ_1 . The cost is based on the squared distance along the curve, made up of the first clothoid length, the second clothoid length and the straight line to the goal at the end.

$$J(\alpha_1, \delta_1) = (s_1 + s_2 + \|\mathbf{x}_G - \tau(L)\|)^2 \quad (15)$$

$$\hat{\alpha}_1, \hat{\delta}_1 = \arg \min_{\alpha_1, \delta_1} J(\alpha_1, \delta_1) \quad (16)$$

subject to

$$\begin{aligned} \tau(0) &= [0, 0, 0, 0] \\ \tau(1) &= [\mathbf{x}_G, 0] \\ \alpha_i &\geq 0 & \forall i \in [1, \dots, n_c] \\ \delta_i &\geq 0 & \forall i \in [1, \dots, n_c] \\ \kappa(p) &\leq \kappa_{max} & \forall p \in [0, L] \\ \alpha(p) &\leq \alpha_{max} & \forall p \in [0, L] \end{aligned} \quad (17)$$

5 PRELIMINARY RESULTS AND DISCUSSION

The two methods were used to estimate the parameters of a transition curve starting at the origin with zero curvature and terminating at $\mathbf{x}_G = [8.000, 6.000, 1.047(60\pi/180)]$. This boundary condition requires two clothoids according to Equation 14.

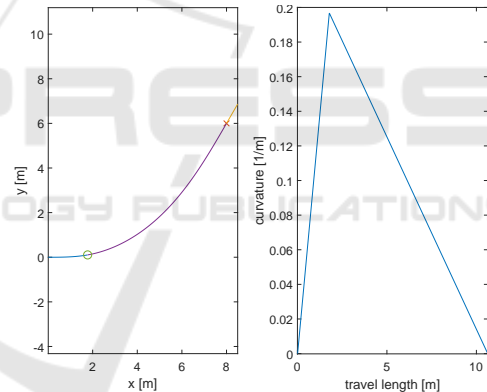


Figure 4: Bisection method: Path output and curvature $[\alpha_1, \delta_1] = [0.0545, 0.6554]$.

The results of the two approaches for a single boundary condition representing a fairly tight left turn of 60 degrees are shown in Table 1 and Figure 4 and 5. Interestingly the estimated parameters are different, resulting in substantially different paths. Both reach the target point with high accuracy and satisfy the constraints to some degree.

Comparing in terms of optimality according to the cost function chosen for the optimization method, the terminal cost of the solution produced by bisection is lower than that produced by fmincon the non-linear constrained optimization tool in MATLAB with much greater computational effort.

The investigation of the cost surface for this single numerical example is seen in Figure 6 to be extremely

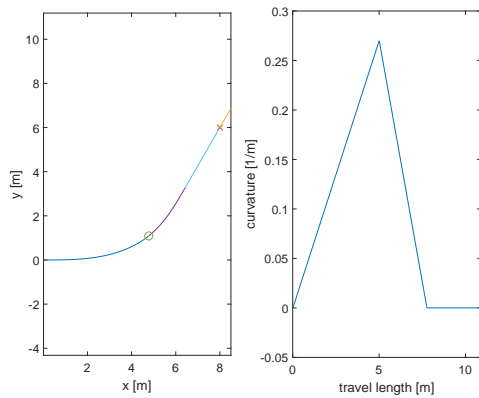


Figure 5: Optimization method: Path output and curvature $[\alpha_1, \delta_1] = [0.1111, 0.1746]$.

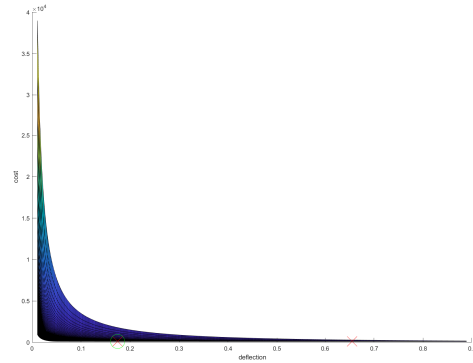


Figure 8: Cost against deflection δ , parameter estimates from both methods shown as red crosses, bisection with a green circle.

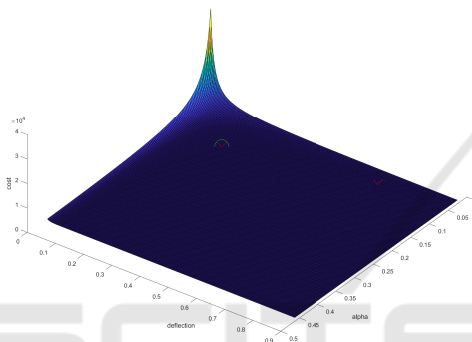


Figure 6: The cost function surface for fmincon with parameter estimates from both methods shown as red crosses, bisection with a green circle.

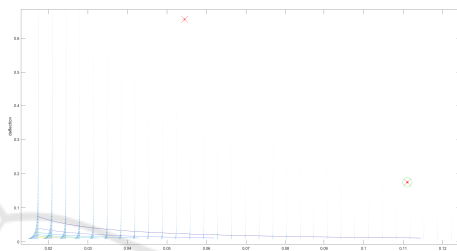


Figure 9: The cost function gradient for fmincon with parameter estimates from both methods shown as red crosses, bisection with a green circle.

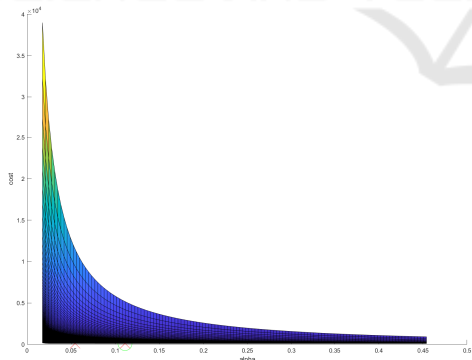


Figure 7: Cost against sharpness α , parameter estimates from both methods shown as red crosses, bisection with a green circle

flat. This causes fmincon to terminate before reaching the optimum based on a step size threshold. It appears that level sets of the cost have a shape close to $y=1/x$ as seen in Figure 9. The path produced by the bisection method is shorter than the one identified by a non-linear constrained optimization where the cost was based on the path length. The different treatment of the constraints permits slightly larger violation by

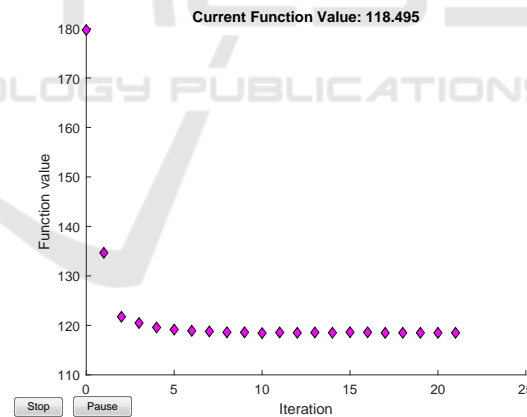


Figure 10: Iterations of fmincon with $\alpha = 0.03$ initial value.

bisection, but this does not adequately explain the significant difference in the resultant path.

To investigate the possibility both methods may have converged to different local minima, both methods were initialized at the minimum reported by the other. The result was that fmincon terminated very close to the bisection minimum, with some constraint violation, the step size threshold preventing further reduction in cost. The evolution for the two initial conditions is shown in Figure 10 and Figure 11. Both terminate due to step size with an infeasible point.

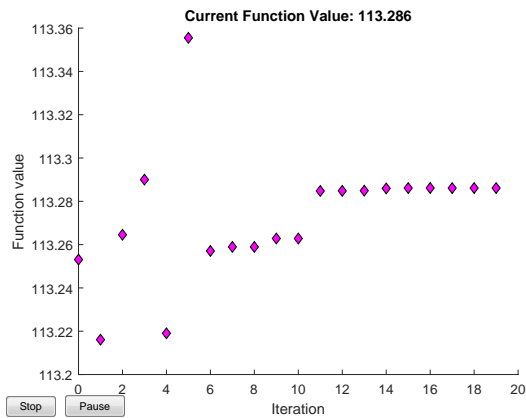


Figure 11: Iterations of fmincon with $\alpha = \hat{\alpha}_{bisection}$ initial value.

Table 1: Comparison table for the two methods.

	fmincon	Bisection
α_1	0.0545	0.1111
δ_1	0.6554	0.1746
Cost	118.4954	113.2531
Path Length	10.8856	10.642
Final Pose		
x	6.477	7.996
y	3.361	5.992
ψ	1.0473	1.0452
κ	-7.992e-05	-1.4731e-04
Constraint Error		
Lateral	2.2751e-05	-4.4731e-06
Heading	-1.4429e-04	2.000e-03
Curvature	-7.992e-05	-1.4731e-04

Bisection, by contrast converged to almost the same point as before when initialized from the fmincon minimum. The impressive stability may be due to the search procedure exploiting the relationship between the input parameters and the error.

6 CONCLUSION

The results presented show the existing bisection method from (Gim et al., 2017) is superior for finding a minimum length, continuous curvature path between an initial and final pose in this case. Violation of heading and curvature constraints is slightly higher, but the solution path length is shorter and the results are more stable to changes in the starting estimate. The potential advantages of restating the problem as a non-linear constrained optimization are not realized because the solver is not able to improve the cost while meeting the constraints. The given optimization approach requires further development such

as a more robust solver which can find a global minimum.

We argue the non-linear constrained optimization formulation is worth pursuing for many applications because other constraints can be applied without having to redesign the heuristic. For example, polygonal obstacle constraints could be included with little modification. The cost function can also be modified to prioritize different aspects such as minimizing curvature rather than path length. Another advantage is the availability of robust general optimization solvers such as ant colony optimization and genetic algorithms which could be employed if necessary to find a global minimum.

7 FURTHER WORK

There is more work to be done tuning the cost function and solver so a stable minimum can be found on this particular example. Beyond this, a range of other simple two-clothoid examples could be generated to show that convergence is consistent. Left and right 90 degree turns of different radius would be sufficient to produce a roadmap approximating a grid. There is no reason to believe the cost surface for the reported case is particularly difficult to solve so investigation of other boundary conditions is important. The next step is to examine the four clothoid case, which allows the creation of ‘lane change’ manoeuvres suitable for overtaking, and then sequences of clothoids forming splines.

One motivation for this work is the reduction of motion sickness for passengers of autonomous vehicles by smooth driving using clothoids. There are numerous approximations to true clothoids which are convenient in some cases, such as polynomial approximation for x and y by Taylor expansion. The use of approximate curves may increase numerical stability, but will result in deviation from the exact clothoid profile. These small curvature discontinuities in the path may or may not be noticeable by passengers. A study where human participants rate their experience when taken on an automated ride using true clothoid curves and approximate ones would provide justification for further work on path generation with the exact integrals.

ACKNOWLEDGEMENTS

This research was made possible thanks to the financial support of a full-time EPSRC Doctoral Training Partnership Studentship - Institute for Transport Studies, and also thanks to the financial support of CASE partner Guidance Automation Limited.

REFERENCES

- Atkinson, K. E. (1988). *An Introduction to numerical analysis, 2nd edition*.
- Beard, G. F. and Griffin, M. J. (2014). Motion sickness caused by roll-compensated lateral acceleration: Effects of centre-of-rotation and subject demographics. *Proceedings of the Institution of Mechanical Engineers, Part F: Journal of Rail and Rapid Transit*, 228(1):16–24.
- Deits, R. and Tedrake, R. (2015). Efficient mixed-integer planning for UAVs in cluttered environments. *Robotics and Automation (ICRA), 2015 IEEE International Conference on*, pages 42–49.
- Dubins, L. E. (1957). On Curves of Minimal Length with a Constraint on Average Curvature, and with Prescribed Initial and Terminal Positions and Tangents. *American Journal of Mathematics*, 79(3):497–516.
- Elsner, J. (2018). Optimizing Passenger Comfort in Cost Functions for Trajectory Planning.
- Fischer, S. (2008). Comparison of railway track transition curves in consideration of clothoid, cosine and wiener bogen transition curves in the respect of the env 13803-1, the Öbb standard and the hungarian railway design regulations (tadr, nrr) in the interval of $v=120 \dots 160$ km/h for normal track gauge.
- Fraichard, T. and Scheuer, A. (2004). From Reeds and Shepp's to Continuous-Curvature Paths. *IEEE Transactions on Robotics*, 20(6):1025–1035.
- Gim, S., Adouane, L., Lee, S., and Dérutin, J. P. (2017). Clothoids Composition Method for Smooth Path Generation of Car-Like Vehicle Navigation. *Journal of Intelligent and Robotic Systems: Theory and Applications*, 88(1):129–146.
- Katrakazas, C., Quddus, M., Chen, W.-H., and Deka, L. (2015). Real-time motion planning methods for autonomous on-road driving: State-of-the-art and future research directions. *Transportation Research Part C: Emerging Technologies*, 60:416–442.
- LaValle, S. M. and Leidner, D. (2006a). Chapter 13: Differential Constraints. In *Planning Algorithms*, chapter 13, pages 715–786. Cambridge University Press.
- LaValle, S. M. and Leidner, D. (2006b). Chapter 3: Geometric Representations and Transformations. In *Planning Algorithms*, chapter 3, pages 81–126. Cambridge University Press.
- Levien, R. (2008). *The Elastica: A Mathematical History*.
- McKenney, W. R. (1970). HUMAN TOLERANCE TO ABRUPT ACCELERATIONS: A SUMMARY OF THE LITERATURE. *Dynamic Science*, 70(13).
- Paden, B., Cap, M., Yong, S. Z., Yershov, D., and Frazzoli, E. (2016). A Survey of Motion Planning and Control Techniques for Self-driving Urban Vehicles. pages 1–27.
- Reeds, J. A. and Shepp, L. A. (1990). Optimal paths for a car that goes forwards and backwards. 145(2):367–393.
- Schwarting, W., Alonso-Mora, J., and Rus, D. (2018). Planning and Decision-Making for Autonomous Vehicles. *Annual Review of Control, Robotics, and Autonomous Systems*, 1(1):annurev-control-060117-105157.
- Siciliano, B. and Khatib, O. (2016). *Robotics and the Handbook*, pages 1–6. Springer International Publishing, Cham.
- Wilde, D. K. (2009). Computing clothoid segments for trajectory generation. *2009 IEEE/RSJ International Conference on Intelligent Robots and Systems, IROS 2009*, pages 2440–2445.
- Zamfir, S., Drosescu, R., and Gaiginschi, R. (2016). Practical method for estimating road curvatures using on-board GPS and IMU equipment. *IOP Conference Series: Materials Science and Engineering*, 147(1).